Mesenchymal stem cells-derived cartilage micropellets: A relevant *in vitro* model for biomechanical and mechanobiological studies of cartilage growth

G. Dusfour[a,1], M. Maumus[b,c,1], P. Cañadas[a], D. Ambard[a], C. Jorgensen[b,c], D. Noël[b,c,2], S. Le Floc'h[a,2,*]

[a] LMGC, Univ. Montpellier, CNRS, Montpellier, France
[b] IRMB, Univ. Montpellier, INSERM, CHU Montpellier, Montpellier, France
[c] Hopital Lapeyronie, Clinical Immunology and Osteoarticular Diseases Therapeutic Unit, Montpellier, France

ABSTRACT

The prevalence of diseases that affect the articular cartilage is increasing due to population ageing, but the current treatments are only palliative. One innovative approach to repair cartilage defects is tissue engineering and the use of mesenchymal stem/stromal cells (MSCs). Although the combination of MSCs with biocompatible scaffolds has been extensively investigated, no product is commercially available yet. This could be explained by the lack of mechanical stimulation during *in vitro* culture and the absence of proper and stable cartilage matrix formation, leading to poor integration after implantation. The objective of the present study was to investigate the biomechanical behaviour of MSC differentiation in micropellets, a well-defined 3D *in vitro* model of cartilage differentiation and growth, in view of tissue engineering applications. MSC micropellet chondrogenic differentiation was induced by exposure to TGFβ3. At different time points during differentiation (35 days of culture), their global mechanical properties were assessed using a very sensitive compression device coupled to an identification procedure based on a finite element parametric model. Micropellets displayed both a non-linear strain-induced stiffening behaviour and a dissipative behaviour that increased from day 14 to day 29, with a maximum instantaneous Young's modulus of 179.9 $\pm$ 18.8 kPa. Moreover, chondrocyte gene expression levels were strongly correlated with the observed mechanical properties. This study indicates that cartilage micropellets display the biochemical and biomechanical characteristics required for investigating and recapitulating the different stages of cartilage development.

1. Introduction

Articular cartilage is a thin tissue that covers the surfaces of long bones in synovial joints. The main biological function of articular cartilage is to allow friction-less movements between the connected bones, while facilitating force transmission. Hence, articular cartilage is a tissue with high mechanical constraints that requires sufficient rigidity to resist mechanical loading, while being able to absorb part of the contact energy between bones. Importantly, articular cartilage is a non-vascularized tissue and this limits its self-repair capacities [1]. In the absence of curative treatments, surgical procedures have been developed to stimulate endogenous regeneration. However, the benefits are non-lasting and the biomechanical properties of the repaired cartilage are generally inferior to those of the original joint. Cell-based

therapeutic options have also been investigated more recently [2]. Mesenchymal stem/stromal cells (MSCs) are likely the best cell source thanks to their accessibility, ease of isolation, high *in vitro* expansion rate and ability to differentiate into chondrocytes [3,4]. *In vitro*, chondrogenic differentiation of MSCs can be induced by culture in alginate beads or in scaffolds [5]. However, the micropellet culture model is currently the standard differentiation assay. Briefly, MSCs are induced to differentiate into chondrocytes after pelleting by centrifugation and are cultured in a chondro-inductive medium that contains Transforming Growth Factor β3 (TGFβ3) [6–8].

As the main function of cartilage is to resist to mechanical stresses, cartilage biomechanical features should be reproduced during *in vitro* differentiation. Many studies on cartilage mechanical properties have focused on the determination of the instantaneous and of the aggregate

---

compression moduli. A recent work determined the *in vivo* intra-tissue strain of femoral and tibial cartilage under cyclic loads that corresponded to 50% of the body weight and found large strains, locally over 10% [9]. Howerver, other studies reported that the actual mechanical load on the knee during walking is much higher than 50% of body load (more than 250%) [10], suggesting that *in vivo* cartilage strain amplitude could be higher than 10% during everyday life movements.

On the other hand, the dissipative and hyperelastic properties of engineered cartilage under large strains have been poorly investigated. Some studies have evaluated the mechanical properties of cartilage scaffolds (see for example [11–13]), but rarely in cartilage micropellets, possibly due to their small size [14,15]. These last two studies demonstrated the interest of atomic force microscopy (AFM) for evaluating the local instantaneous elastic modulus and showed that micropellets possess some characteristics of native cartilage, suggesting that cartilage micropellets could be relevant *in vitro* models for biomechanical analysis of articular cartilage. However, the mechanical properties of micropellets were not investigated at different time points, but only at the end of chondrogenic differentiation. Moreover, the micropellet global properties, and their hyperelastic and dissipative behaviour (*i.e.*, the capacity of articular cartilage to undergo large deformation and to dampen mechanical loads) were not analysed.

The present study investigated whether MSC-derived cartilage micropellets reproduce the main biomechanical features of native articular cartilage in order to confirm the relevance of this 3D model for cartilage growth studies. To this aim, the global hyperelastic and dissipative properties of micropellets obtained from MSCs cultured in aggregates in the presence of TGFβ3 were investigated during 5 weeks of culture as well as the temporal expression profile of cartilage-specific genes.

2. Materials and methods

2.1. MSC isolation and chondrogenic differentiation

Human MSCs were isolated from the bone marrow of one 82-year-old male patient who underwent hip replacement surgery after informed consent and approval by the local ethics committee (registration number: DC-2009-1052). MSCs were characterized by the expression of classical markers (CD13, CD73, CD90, and CD105), the absence of hematopoietic and endothelial markers (CD11b, CD14, CD31, CD34, and CD45), and their differentiation potential (differentiation into adipocytes, osteoblasts and chondrocytes, as described in [16]) (data not shown). Chondrogenic differentiation was induced using the micropellet model by centrifuging 2.5×10^5 MSCs at 300 g for 5 min in 15 ml conical tubes. Chondrogenic medium (DMEM high glucose, dexamethasone 0.1 μM, sodium pyruvate 1 mM, ascorbic-2-phosphate acid 170 μM, ITS 1% (insulin/transferrin/selenic acid), proline 0.35 mM), supplemented with 10 ng/ml TGFβ3 or not (negative control) (Bio-Techne, Lille) was changed every 3 days. At different time points (day 7, 14, 21, 29 or 35), micropellets were washed in phosphate buffered saline (PBS) and immediately processed for mechanical characterization, or fixed for 1 h in 4% formaldehyde for immunohistochemical analysis or stored at −80 °C for RT-qPCR analysis.

2.2. RT-qPCR

Total RNA was extracted from micropellets using the RNeasy Kit (Qiagen, Courtaboeuf). RNA (0.5 μg) was reverse transcribed using the M-MLV reverse transcriptase (ThermoFisher scientific, Villebon-sur-Yvette). Primers for chondrocyte markers were designed using the Primer3 software (sequences in Table 1) and purchased from MWG (Eurofinsgenomics, Courtaboeuf). PCR reactions were carried out using 10 ng of cDNA, 5 μmol/L of each primer, and 5 μL 2× SybrGreen PCR Master Mix (Roche, Meylan). The following cycling conditions were used: 95 °C for 5 min; then 40 cycles at 95 °C for 15 s; 64 °C for 10 s and

72 °C for 20 s in a Viia7 Real-Time PCR System (Life Technologies, Courtaboeuf). Results were analysed with the dedicated software. All values were normalized to the housekeeping gene RPS9 and expressed as relative expression or fold change using the respective formula $2^{-\Delta CT}$ or $2^{-\Delta\Delta CT}$.

2.3. Immunohistochemical analysis

Micropellets were processed for routine histology. Deparaffinised micropellet sections (3 μm) were stained with Safranin O/Fast Green for proteoglycan visualization in orange. Immunohistochemistry was performed using anti-aggrecan (1/1000 dilution; Chemicon, Millipore, Molsheim) and anti-type II collagen (1/50 dilution; Lab Vision, Francheville) antibodies and the Lab Vision UltraVision Detection System anti-Polyvalent HRP/DAB Kit (Lab Vision). Sections were counter-stained with Mayer's haematoxylin (Lab Vision) for 3 min and mounted with Eukitt (Sigma-Aldrich, Lyon).

2.4. Mechanical compression tests

A total of 53 micropellets were individually characterized at different stages of MSC differentiation (day 7, 14, 21, 29 and 35). After removal of the culture medium, each micropellet was kept in 5 ml of phosphate buffered saline (PBS) at room temperature (22 °C ± 1 °C) until analysis to estimate the apparent (*i.e.* instantaneous, dynamic) mechanical properties. Each micropellet was placed between platens for overall compression that consisted in 1 cycle of compression with an imposed displacement of 200 μm for a total duration of 1 s. A constant speed for the compression and for returning to the initial position was used (Fig. 1A–B). The chosen displacement amplitude and rate mimicked the strain experienced by joints during walking, as reported by recent *in vivo* studies [9,10]. The force and displacement were acquired simultaneously at 100 Hz. The force was measured with a miniature S Beam load cell (Futek Inc., model LSB200, Irvine, USA).

2.5. Determination of the dissipated energy

The difference between the integral of the increasing force along the displacement during the compression phase and the integral of the decreasing force along the displacement during the return to the initial state allowed computing the dissipated energy for the complete cycle.

2.6. Identification of the hyperelastic properties

The micropellet hyperelastic properties were also estimated by implementing a hyperelastic density energy model, as proposed by Fung [17] coupled with a finite element (FE) model of a deformable sphere using the LMGC90 software [18]. The constitutive isotropic hyperelastic behaviour of micropellets was described using the Fung's formula to determine the strain energy function:

$$\Psi_{fung} = \frac{E}{4b(1+v)}e^{b(I_1-3)}$$

where E is the Young's modulus that represents the initial micropellet stiffness at small strains, v is the Poisson's ratio, and b a parameter corresponding to the sample strain-stiffening behaviour. A quasi-incompressible behaviour was implemented with a Poisson's ratio v of 0.499. Indeed, it was assumed that the strain rate was high enough during unconfined compression to consider the micropellet as quasi-incompressible [19].

For each tested micropellets, a quarter of a circle using axisymmetric modelling was meshed using GMSH (Fig. 1C) [20]. After analysis of the convergence of the solution with the number of elements, 3696 linear quadrangles were necessary. A contact law without friction was used between the rigid compression platen and the deformable sphere. The finite element model was implemented in a parametric manner as

Table 1
Primer sequences.

Gene symbol	Gene name	Sequence forward	Sequence reverse
ACAN	Aggrecan	TCGAGGACAGCGAGGCC	TCGAGGGTGTAGCGT-GTAGAGA
ALPL	Alkalin phosphatase	CCACGTCTTCACATT-TGGTG	GCAGTGAAGGGCTTC-TTGTC
COL10A1	Collagen type X	TGCTGCCACAAATAC-CCTTT	GTGGACCAGGAGTAC-CTTGC
COL2A1ΔB	Collagen type IIB	CAGACGCTGGTGCTGCT	TCCTGGTTGCCGGACAT
HAPLN1	Link protein	TTCCACAAGCACAAA-CTTTACACAT	GTGAAACTGAGTTTT-GTATAACCTCTCAGT
RSP9	Ribosomal small protein 9	ATGAAGGACGGGATG-TTCAC	GATTACATCCTGGGC-CTGAA
SOX9	Sex Determining Region Y-Box 9	AGGTGCTCAAAGGCT-ACGAC	GTAATCCGGGTGGTC-CTTCT

such that the radius, the Young's modulus and the parameter b could be tuned. A non-linear minimization procedure (*least_square* from the *scipy.optimize* module, with a Trust Region algorithm, in *python*) was used to fit the force from the FE model to the experimental force, in order to identify the Young's modulus E and the parameter b.

2.7. Statistical analysis

All data are presented as the mean ± standard error of the mean (SEM). The number of tested samples varied from six to eight, depending on the experiment. All mechanical values (E and b) were recorded in a spreadsheet according to the presence or absence of TGFβ3, time point, and date of the mechanical evaluation. As the data did not adopt a Gaussian distribution, non-parametric statistical tests were used. Two groups were compared using the Mann-Whitney test. The Kruskal-Wallis test followed by the Dunn's multiple comparison test was used to compare three or more groups. Correlations were analysed using the non-parametric Spearman correlation test. The test used is indicated in the figure legend.

3. Results

3.1. TGFβ3-induced MSC derived cartilage micropellets exhibit strain-induced stiffening and dissipative behaviour

RT-qPCR analysis of cartilage-specific genes was performed at day 0 (D0; before differentiation) and at D21 after MSC culture in micropellets in the presence or absence of TGFβ3. At D21, expression of SOX9, type IIB collagen (COL2A1ΔB) and aggrecan (ACAN) was significantly higher in micropellets cultured with TGFβ3 than in MSCs at D0 or in D21 undifferentiated micropellets cultured without TGFβ3 (Fig. 2A). Similarly, the micropellet diameter at D21 was significantly higher in differentiated (+TGFβ3) than undifferentiated (−TGFβ3) micropellets (Fig. 2B), corresponding to an increase of 57% of the micropellet volume.

Moreover, at D21, the Young's modulus, estimated using the sample-specific FE model, was 5.3-fold higher in differentiated micropellets

(160.4 ± 17.5 kPa) compared with undifferentiated samples (32.8 ± 8.3 kPa, $p < 0.001$) (Fig. 2C). The high values of parameter b (10.5 ± 0.8 kPa) indicated a strong strain-stiffening behaviour of differentiated micropellets. As shown in Fig. 2E, the linear elastic Hertzian contact model was not able to describe the micropellet non-linear behaviour. This was partly explained by the violation of the hypotheses on which is based the Hertzian contact theory. An additional numerical investigation, which used a neo-Hookean model of strain energy function, showed that this inability was mostly due to the micropellet strain-stiffening behaviour (data not shown).

A representative behaviour of a differentiated micropellet during a complete cycle of loading (*i.e.*, compression - return to initial state) is shown in Fig. 2F. The hysteresis area revealed a strong dissipative behaviour. At D21, the dissipated energy of differentiated micropellets (+TGFβ3) was 3.4 fold higher than that of undifferentiated micropellets (−TGFβ3) ($307 \pm 46 \times 10^{-9}$ J *versus* $88 \pm 24 \times 10^{-9}$ J, $p < 0.05$) (Fig. 2D).

These biochemical, geometrical and mechanical analyses demonstrated that upon addition of TGFβ3, MSCs differentiated into chondrocytes that produced a ECM with the expected strain-stiffening and dissipative properties of cartilage. Therefore, the other analyses were performed using only TGFβ3-induced cartilage micropellets.

3.2. The micropellet mechanical and geometrical properties gradually increase with the production of cartilage matrix

Then, the micropellet mechanical behaviour and the production of cartilage-specific ECM were monitored during MSC differentiation into chondrocytes upon exposure to TGFβ3. Expression of chondrocyte-specific genes gradually increased from D0 to D35 (Fig. 3A). As expected, expression of the transcription factor SOX9, responsible for the expression of chondrocyte markers, was induced at D7 and then decreased until D21 before increasing again at D35. All other markers gradually increased from D14 or D21 until D29 or D35. Type X collagen (COL10A1) and alkaline phosphatase (ALPL), two markers of hypertrophic chondrocytes, progressively increased up to D35. COL2A1ΔB and the gene encoding hyaluronan and proteoglycan link protein 1
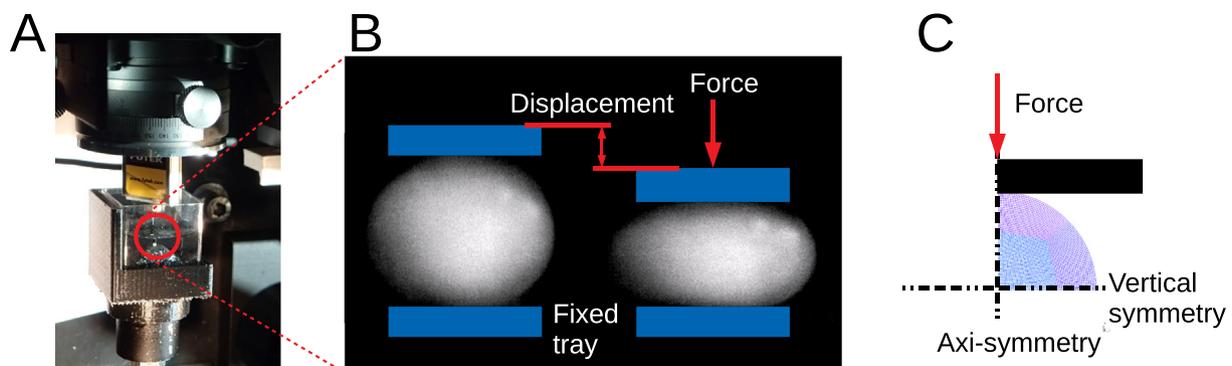

Fig. 1. Global compression test on micropellets. (A) Image of the device used for the mechanical characterization. (B) Schematic representation of the compression test (exaggerated deformation). (C) Symmetry assumptions used with the Finite Element model to estimate the micropellet hyperelastic properties.
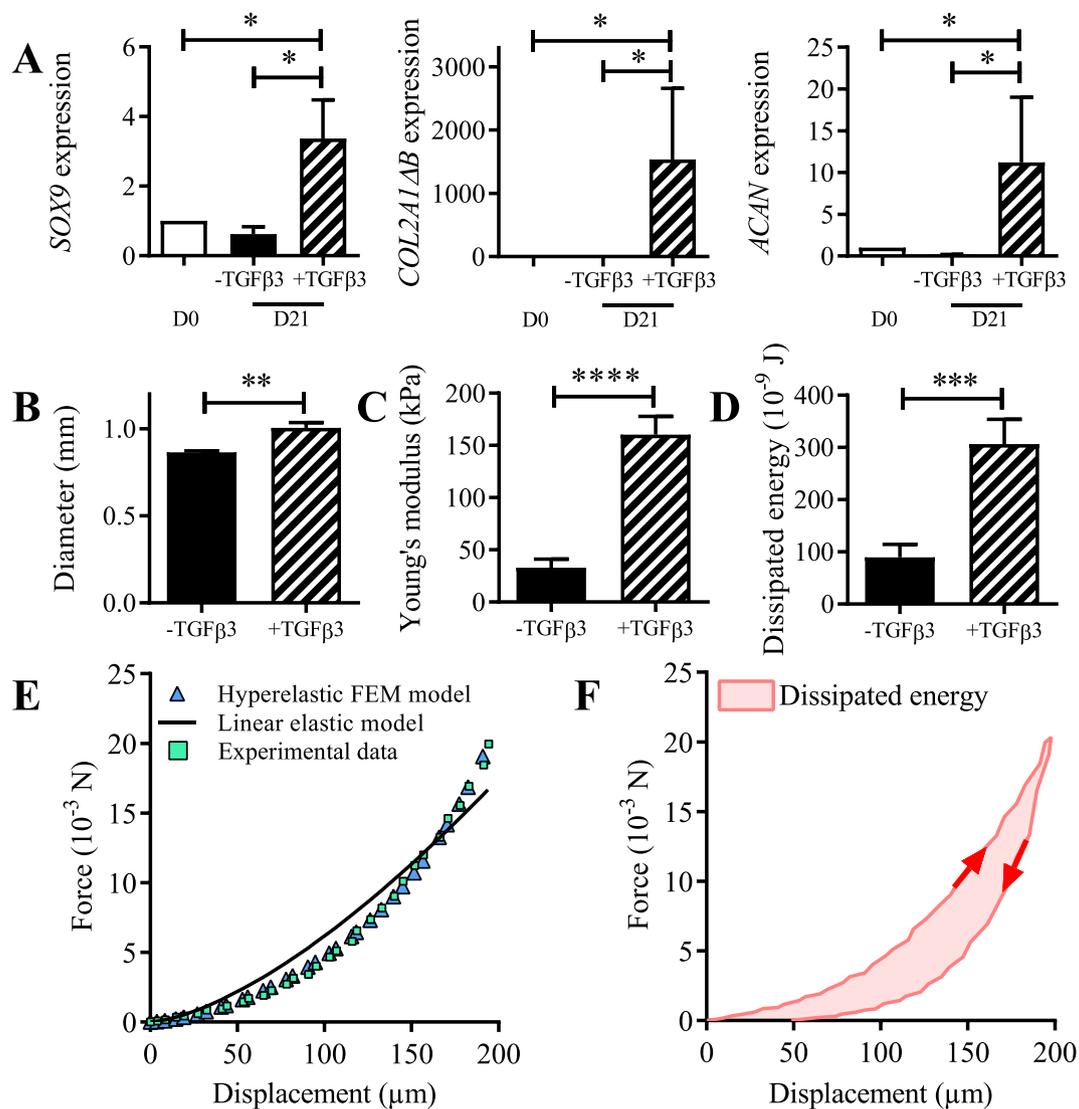
Fig. 2. Differentiation and mechanical characterization of micropellets cultured with or without TGFβ3. (A) Gene-expression of SOX9, type IIB collagen (COL2BA1ΔB) and aggrecan (ACAN) measured by RT-qPCR (n = 3). (B) Mean diameters of micropellets cultured with or without TGFβ3 (n = 13). (C) Young's modulus estimated from a hyperelastic Finite Element model on same micropellets (n = 13). (D) Dissipated energy during the compression tests (n = 13). (E) Plot of the force as a function of the displacement during the compression test, exhibiting the strain-stiffening behaviour; experimental data from micropellets differentiated with TGFβ3 in B–D are represented by squares, the linear Hertz model fit by the solid line and the hyperelastic Finite element model fit by the triangles. (F) Plot of the force as a function of the displacement for the complete compression cycle, exhibiting energy dissipation characterized through the hysteresis. Statistical analysis used a Mann-Whitney test: $*p < 0.05$, $**p < 0.01$, $***p < 0.001$ and $****p < 0.0001$.

(HAPLN1) increased from D0 to D29, and then decreased to levels that remained well above those of D0. ACAN expression gradually increased from D7 to D35, although its basal level was already high in MSCs at D0. Immunohistological analysis of micropellets at different time points after chondrogenesis induction confirmed the production of ECM proteins (Fig. 3B). Safranin O/Fast green staining highlighted the progressive accumulation of proteoglycans (orange/red colour) starting from D21. Moreover, antibodies against type IIB collagen and aggrecan revealed the accumulation of these proteins from D21 to the end of the experiment. This analysis confirmed that in micropellet culture, MSCs differentiated into chondrocytes by D21 and that longer culture times were required to increase the cartilage growth and ECM production. Finally, evaluation of the micropellet mechanical properties showed that the micropellet diameter increased significantly between D21 and D29, corresponding to a 29% increase of their volume (Fig. 3C). After 7 days of culture in the presence of TGFβ3 (D7), the micropellet mechanical strength was insufficient to resist to the compression test. Conversely, the micropellets Young's modulus significantly increased

from D14 to D29 (from 12.1 ± 2.3 kPa to 179.9 ± 18.8 kPa), and then was stabilized at 168.9 ± 28.6 kPa at D35 (Fig. 3D). The value of parameter b (indicative of the micropellet non-linear behaviour) increased from D14 to D21, (respectively 3.8 ± 2.3 and 12.4 ± 1.1, $p < 0.01$), and then seemed to oscillate until day 35 (16.1 ± 1.1, $p < 0.05$). Like the Young's modulus, the dissipated energy progressively increased until D29 and then remained stable up to D35 (226 ± 39 × 10^{-9} J) (Fig. 3E). The micropellet dissipative behaviour remained rather constant over time with an average ratio between dissipated energy and elastic energy of 46.5 ± 8% during the compression cycle.

3.3. The micropellet hyperelastic and dissipative properties are correlated with chondrocyte gene expression level

Remarkably, a significant correlation between gene expression and mechanical properties was observed. The expression of HAPLN1 and COL2A1ΔB was significantly correlated with the Young's modulus,
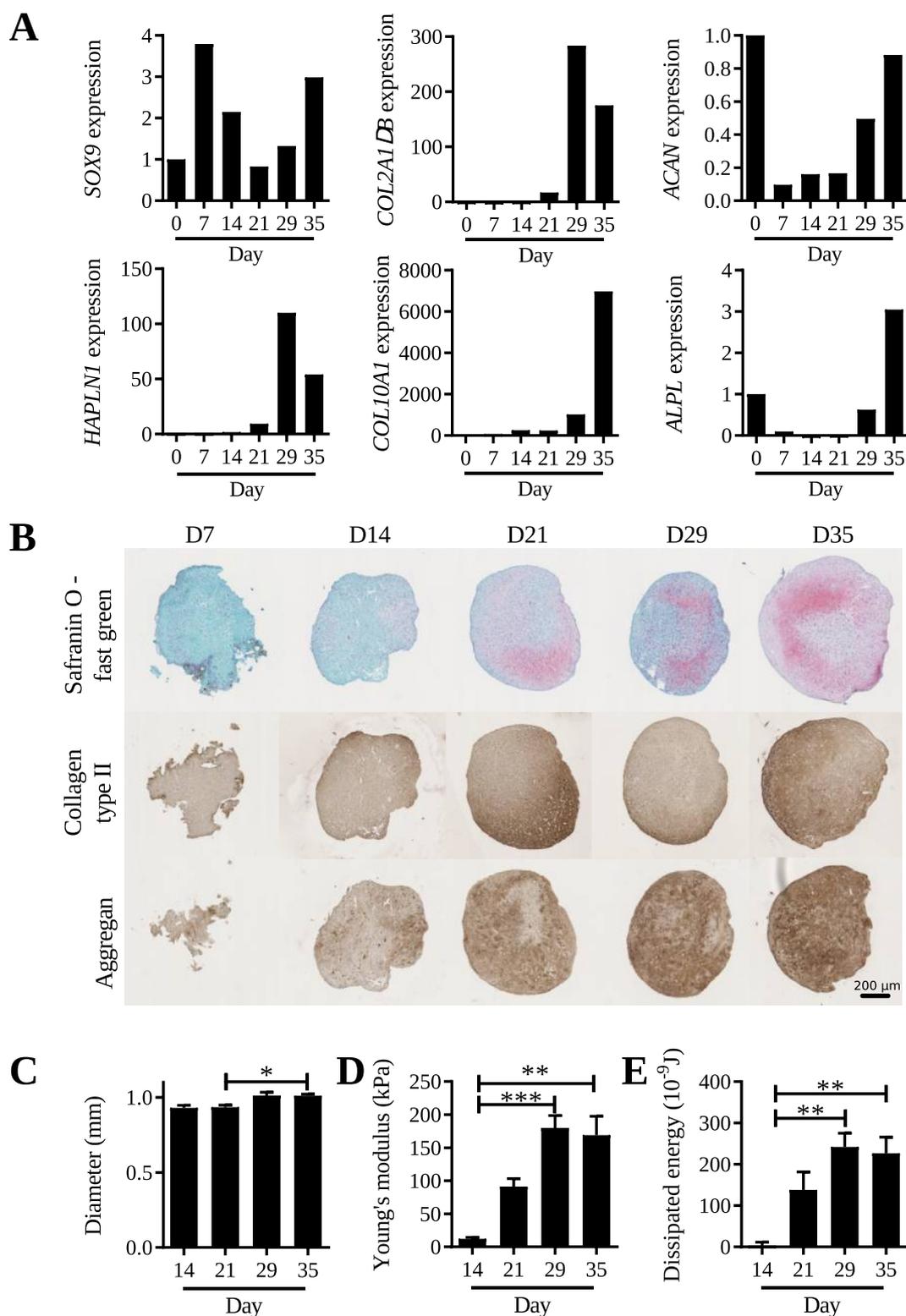
Fig. 3. Differentiation and mechanical characterization of MSC micropellet culture using TGFβ3, at different days. (A) Gene expression measured by RT-qPCR from day 0 to day 35 during the differentiation of MSC in micropellets (HAPLN1 for Link protein, COL10A1 for type X collagen and ALPL for alkaline phosphatase) (n = 1 replicate of 7 pooled micropellets). (B) Histological and immunohistological staining of proteoglycans (Safranin O fast green; upper panels), type II Collagen (middle panels) and aggrecan (lower panels). (C) Mean diameter of micropellets at different time points, (D) Young's modulus and (E) dissipated energy during the compression cycle from day 14 to day 35 on same micropellets (n = 7 for each time point). Statistical analysis used a Kruskal-Wallis test followed by Dunn's post-test: *p < 0.05, **p < 0.01 and ***p < 0.001. (For interpretation of the references to color in this figure, the reader is referred to the web version of this article.)
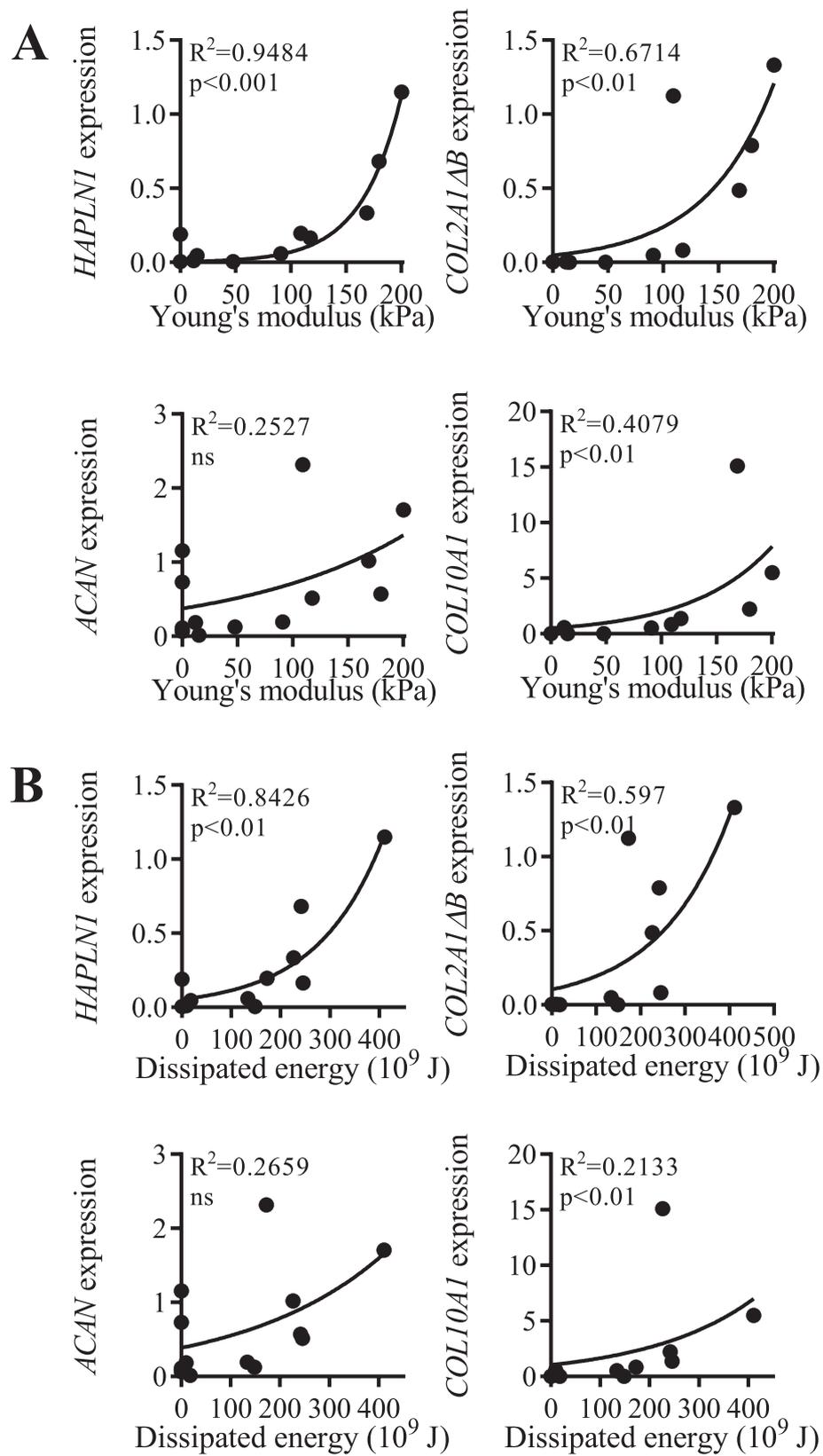
Fig. 4. Correlation between the expression levels of different chondrocyte genes and the mechanical properties of micropellets at day 21. (A) Gene expression as a function of the Young's modulus (n = 13). (B) Gene expressions as a function of the dissipated energy (n = 13). Statistical analysis used Spearman correlation test; ns, not significant.

estimated using the Fung strain energy density formula (Fig. 4A). Interestingly, when the expression of chondrogenic genes decreased at day 35, the associated Young's modulus also tended to decrease (Fig. 3A and D). Conversely, expression of ACAN and COL10A1 (a marker of hypertrophic chondrocytes) was not significantly correlated with the micropellet mechanical properties. Similar results were obtained for the relationship between dissipated energy and chondrogenic markers (Fig. 4B). These results indicated that the expression level of HALPN1 and COL2A1ΔB is an indicator of the cartilage micropellet stiffness and dissipative behaviour. Conversely, SOX9 expression was not correlated with the measured mechanical properties (data not shown), possibly due to its main role as inducer of cartilage-specific genes.

4. Discussion

In the present study, we demonstrated that MSC-derived cartilage micropellets upon exposure to TGFβ3 display similar qualitative mechanical behaviour as native cartilage. In the absence of TGFβ3, MSC pellets did not differentiate into chondrocytes and did not secrete the specific cartilaginous ECM, as shown by absence of chondrogenic gene expression and weak resistance to mechanical stress.

Native articular cartilage is a soft tissue with a biphasic structure displaying a hyperelastic dissipative behaviour [21,22]. Its hyperelastic behaviour ensures mechanical integrity upon large strains, while its dissipative behaviour guarantees the role of mechanical damper or shock absorber in joints. Therefore, it is not surprising that the analytical Hertzian contact model between a linear elastic sphere and a rigid platen could not properly estimate the micropellet behaviour for displacements bigger than 50 μm, for which the assumptions used in the Hertzian theory are no longer verified. Conversely, the hyperelastic FE model took into account the stiffening behaviour of cartilage micropellets. The experimental results also showed a strong dissipative behaviour, with a ratio between the dissipated energy and the elastic energy of 46.5% during the compression cycle. In studies on the viscoelastic properties of human articular cartilage, the ratio between the loss modulus (associated with the dissipated energy) and the storage modulus (associated with the elastic energy) ranged between 5% and 25% at 1 Hz [23–25]. At the cellular level, the viscoelastic properties of human chondrocytes also revealed a strong dissipative behaviour [26–28]. The dissipation of mechanical energy might be explained by the tissue biphasic nature, and this hypothesis could be assessed in future studies using cartilage micropellets.

In the present study, the Young's modulus of cartilage micropellets (179.9 kPa) was 7.2–9.0- and 6.0-fold higher than the values obtained for cartilage micropellets differentiated from induced pluripotent stem cells and from nasal chondrocytes using AFM indentation tests (20–25 kPa and 30 kPa, respectively) [14,15]. In our study, global compression experiments were performed at the millimetric scale (*i.e.*, global compression of the micropellet), whereas AFM indentation tests were performed at the micrometric (25 μm tip) and nanometric (20 nm tip) scales (*i.e.*, local compression of micropellet cross-sections). As clearly outlined in another report [29], one order of magnitude differences could be observed depending on the indenter size, and this might explain the differences observed among studies. In addition, also the cells used for generating the micropellets could contribute to the differences in Young's modulus values. Indeed, ECM content and microstructural organization could significantly differ in micropellets derived from MSCs, pluripotent stem cells, and nasal chondrocytes.

Moreover, the instantaneous (*i.e.*, dynamic, apparent) macroscopic elastic modulus of native human articular cartilage estimated in previous studies using similar strain rates was one to two orders of magnitude higher than the Young's modulus of cartilage micropellets found in our study (see review [23] and more specifically [22,24,25,29–36]). The elastic response of cartilage micropellets is more similar to the response of surface cartilage of new-born animals [37,38], suggesting that the produced ECM had not reached histological/mechanical

maturity yet.

Several studies in animal models [39–43] demonstrated that the instantaneous elastic modulus increases during growth, until reaching a peak at skeletal maturity. In the present study, the radius (*i.e.*, volume), the instantaneous Young's modulus, the dissipated energy, and the strain-stiffening behaviour (parameter b) of cartilage micropellets increased until reaching a plateau at D29 of culture. This suggests a change in the remodelling and developmental processes. Similarly, the expression of chondrocyte genes decreased after D29, while the expression of hypertrophic chondrocyte phenotype markers increased. In addition, our histological analysis showed a non-homogeneous production of ECM components. Safranin O/Fast green staining and type II collagen proteins accumulated more at the periphery than at the centre of the micropellets. This might be explained by the lack of (or lower) diffusion of nutrients from the culture medium to the micropellet centre. Previous biochemical studies [44–46] and micro-indentation studies reported spatially heterogeneous cell phenotype and mechanical behaviours, highlighting the difficulty to obtain homogeneous cartilage micropellets [14,15]. Interestingly, a study showed that the spatial homogeneity of type II collagen and proteoglycan expression in cartilage micropellets can be improved by increasing glucose concentration in the culture medium. This suggests that chondrogenesis in the micropellet centre could be promoted by increasing the nutrient-containing flux circulation [47].

Despite these limitations, the 3D micropellet model is considered the most relevant model for *in vitro* cartilage formation. Indeed, it recapitulates the early phases of MSC differentiation from the condensation step to the generation of chondroprogenitors, chondroblasts, chondrocytes and hypertrophic chondrocytes. In our study, MSC chondrogenic differentiation was associated with an increase of the micropellet volume and a drastic gain of mechanical properties during the first weeks of culture, indicating important modifications of the cartilaginous matrix microstructure. Moreover, chondrocyte gene expression increased between D14 and D29, in parallel with the increase of mechanical strength and extracellular volume production.

Modulation of gene expression reflects the cell response to environmental clues, particularly the local cell environment stiffness that induces cell differentiation through the mechanosensing machinery [48]. A study demonstrated that both TGFβ3 and ECM stiffness are required for promoting chondrocyte differentiation and that mechanosensitive chondro-induction is mediated by ROCK signalling [49]. The correlations between chondrogenic gene expression and mechanical properties in our study may suggest that mechanosensitive chondro-induction guided the formation of cartilage micropellets.

5. Conclusions

Using a very sensitive dedicated device for mechanical testing of cartilage objects, the present study demonstrated that chondrocyte gene expression and extracellular matrix mechanical stiffness changes are correlated during chondrogenic differentiation of MSC micropellets. This suggests that cartilage micropellets are a good *in vitro* biomechanical model of cartilage growth. Indeed, the cartilage micropellet model displays the biochemical and biomechanical characteristics that recapitulate the different stages of cartilage development and are required for experimental studies. Future studies should combine analysis of the mechanotransduction pathways [49] and mechanobiological models [50,51] to improve our understanding of mature cartilage formation.

CRediT authorship contribution statement

G. Dusfour: Investigation, Formal analysis, Writing - original draft, Software. **M. Maumus:** Investigation, Formal analysis, Visualization, Validation. **P. Cañadas:** Project administration, Writing - review & editing. **D. Ambard:** Software. **C. Jorgensen:** Resources. **D. Noël:**

Methodology, Conceptualization, Supervision, Writing - original draft. **S. Le Floc'h:** Methodology, Conceptualization, Supervision, Writing - original draft, Software.

Declaration of competing interest

There are no known conflicts of interest associated with this publication and there has been no significant financial support for this work that could have influenced its outcome.

References

[1] D.J. Huey, J.C. Hu, K.A. Athanasiou, Unlike bone, cartilage regeneration remains elusive, Science 338 (6109) (2012) 917–921, https://doi.org/10.1126/science. 1222454.

[2] J.W. Alford, B.J. Cole, Cartilage restoration, part 1: basic science, historical perspective, patient evaluation, and treatment options, Am. J. Sports Med. 33 (2) (2005) 295–306, https://doi.org/10.1177/036354650427351.

[3] B.M. Davies, S.J.B. Snelling, L. Quek, O. Hakimi, H. Ye, A. Carr, A.J. Price, Identifying the optimum source of mesenchymal stem cells for use in knee surgery, J. Orthop. Res. 35 (9) (2017) 1868–1875, https://doi.org/10.1002/jor.23501.

[4] C. De Bari, A.J. Roelofs, Stem cell-based therapeutic strategies for cartilage defects and osteoarthritis, Curr. Opin. Pharmacol. 40 (2018) 74–80, https://doi.org/10. 1016/j.coph.2018.03.009.

[5] C. Vinatier, C. Mrugala, C. Jorgensen, J. Guicheux, D. Noël, Cartilage engineering: a crucial combination of cells, biomaterials and biofactors, Trends Biotechnol. 27 (5) (2009) 307–314.

[6] B. Johnstone, T.M. Hering, A.I. Caplan, V.M. Goldberg, J.U. Yoo, In vitro chondrogenesis of bone marrow-derived mesenchymal progenitor cells, Exp. Cell Res. 238 (1) (1998) 265–272, https://doi.org/10.1006/excr.1997.3858.

[7] J. Yoo, T. Barthel, K. Nishimura, L. Solchaga, A. Caplan, V. Goldberg, B. Johnstone, The chondrogenic potential of human bone-marrow-derived mesenchymal progenitor cells, J. Bone Joint Surg. 80 (12) (1998) 1745–1757.

[8] H. Rogan, F. Ilagan, F. Yang, Comparing single cell versus pellet encapsulation of mesenchymal stem cells in three-dimensional hydrogels for cartilage regeneration, Tissue Eng. A 25 (19–20) (2019) 1404–1412, https://doi.org/10.1089/ten.tea. 2018.0289.

[9] D.D. Chan, L. Cai, K.D. Butz, S.B. Trippel, E.A. Nauman, C.P. Neu, *In vivo* articular cartilage deformation: noninvasive quantification of intratissue strain during joint contact in the human knee, Sci. Rep. 6 (2016) 19220, , https://doi.org/10.1038/ srep19220.

[10] I. Kutzner, B. Heinlein, F. Graichen, A. Bender, A. Rohlmann, A. Halder, A. Beier, G. Bergmann, Loading of the knee joint during activities of daily living measured in vivo in five subjects, J. Biomech. 43 (11) (2010) 2164–2173, https://doi.org/10. 1016/j.jbiomech.2010.03.046.

[11] L. Bian, K. Ng, E. Lima, D. Xu, P. Jayabalan, G. Ateshian, A. Stoker, J. Cook, C. Hung, Applied dynamic loading enhances mechanical properties of engineered cartilage using adult chondrocytes, Trans. Orthop. Res. 35 (2010) 0382.

[12] S. Grad, M. Loparic, R. Peter, M. Stolz, U. Aebi, M. Alini, Sliding motion modulates stiffness and friction coefficient at the surface of tissue engineered cartilage, Osteoarthr. Cartil. 20 (4) (2012) 288–295, https://doi.org/10.1016/j.joca.2011.12. 010.

[13] D.J. Griffin, E.D. Bonnevie, D.J. Lachowsky, J.C. Hart, H.D. Sparks, N. Moran, G. Matthews, A.J. Nixon, I. Cohen, L.J. Bonassar, Mechanical characterization of matrix-induced autologous chondrocyte implantation (MACI®) grafts in an equine model at 53 weeks, J. Biomech. 48 (10) (2015) 1944–1949, https://doi.org/10. 1016/j.jbiomech.2015.04.010.

[14] B.O. Diekman, N. Christoforou, V.P. Willard, H. Sun, J. Sanchez-Adams, K.W. Leong, F. Guilak, Cartilage tissue engineering using differentiated and purified induced pluripotent stem cells, Proc. Natl. Acad. Sci. 109 (47) (2012)

[15] L. Peñuela, F. Wolf, R. Raiteri, D. Wendt, I. Martin, A. Barbero, Atomic force microscopy to investigate spatial patterns of response to interleukin-1beta in engineered cartilage tissue elasticity, J. Biomech. 47 (9) (2014) 2157–2164, https:// doi.org/10.1016/j.jbiomech.2013.10.056.

[16] A.T. Maria, K. Toupet, M. Maumus, G. Fonteneau, A. Le Quellec, C. Jorgensen, P. Guilpain, D. Noël, Human adipose mesenchymal stem cells as potent anti-fibrosis therapy for systemic sclerosis, J. Autoimmun. 70 (2016) 31–39, https://doi.org/10. 1016/j.jaut.2016.03.013.

[17] Y. Fung, Elasticity of soft tissues in simple elongation, Am. J. Phys. 213 (6) (1967) 1532–1544.

[18] F. Dubois, R. Mozul, LMGC90, 13e Colloque National En Calcul Des Structures, Université Paris-Saclay, Giens, Var, France, 2017.

[19] G.A. Ateshian, B.J. Ellis, J.A. Weiss, Equivalence between short-time biphasic and incompressible elastic material responses, J. Biomech. Eng. 129 (3) (2007) 405–412, https://doi.org/10.1115/1.2720918.

[20] C. Geuzaine, J.-F. Remacle, Gmsh: a 3-D finite element mesh generator with built-in pre-and post-processing facilities, Int. J. Numer. Methods Eng. 79 (11) (2009) 1309–1331.

[21] V.C. Mow, M.H. Holmes, W.M. Lai, Fluid transport and mechanical properties of articular cartilage: a review, J. Biomech. 17 (5) (1984) 377–394, https://doi.org/ 10.1016/0021-9290(84)90031-9.

[22] K. Athanasiou, M. Rosenwasser, J. Buckwalter, T. Malinin, V. Mow, Interspecies comparisons of in situ intrinsic mechanical properties of distal femoral cartilage, J. Orthop. Res. 9 (3) (1991) 330–340, https://doi.org/10.1002/jor.1100090304.

[23] C.J. Little, N.K. Bawolin, X. Chen, Mechanical properties of natural cartilage and tissue-engineered constructs, Tissue Eng. B Rev. 17 (4) (2011) 213–227.

[24] D.K. Temple, A.A. Cederlund, B.M. Lawless, R.M. Aspden, D.M. Espino, Viscoelastic properties of human and bovine articular cartilage: a comparison of frequency-dependent trends, BMC Musculoskelet. Disord. 17 (1) (2016) 419.

[25] M. Ebrahimi, S. Ojanen, A. Mohammadi, M.A. Finnilä, A. Joukainen, H. Kröger, S. Saarakkala, R.K. Korhonen, P. Tanska, Elastic, viscoelastic and fibril-reinforced poroelastic material properties of healthy and osteoarthritic human tibial cartilage, Ann. Biomed. Eng. (2019) 1–14.

[26] W.R. Trickey, G.M. Lee, F. Guilak, Viscoelastic properties of chondrocytes from normal and osteoarthritic human cartilage, J. Orthop. Res. 18 (6) (2000) 891–898.

[27] E.M. Darling, M. Topel, S. Zauscher, T.P. Vail, F. Guilak, Viscoelastic properties of human mesenchymally-derived stem cells and primary osteoblasts, chondrocytes, and adipocytes, J. Biomech. 41 (2) (2008) 454–464.

[28] B.V. Nguyen, Q.G. Wang, N.J. Kuiper, A.J. El Haj, C.R. Thomas, Z. Zhang, Biomechanical properties of single chondrocytes and chondrons determined by micromanipulation and finite-element modelling, J. R. Soc. Interface 7 (53) (2010) 1723–1733.

[29] M. Stolz, R. Gottardi, R. Raiteri, S. Miot, I. Martin, R. Imer, U. Staufer, A. Raducanu, M. Düggelin, W. Baschong, et al., Early detection of aging cartilage and osteoarthritis in mice and patient samples using atomic force microscopy, Nat. Nanotechnol. 4 (3) (2009) 186, https://doi.org/10.1038/NNANO.2008.41.

[30] G. Kempson, M. Freeman, S. Swanson, The determination of a creep modulus for articular cartilage from indentation tests on the human femoral head, J. Biomech. 4 (4) (1971) 239–250.

[31] C. Armstrong, V. Mow, Variations in the intrinsic mechanical properties of human articular cartilage with age, degeneration, and water content, J. Bone Joint Surg. Am. 64 (1) (1982) 88–94.

[32] A. Swann, B. Seedhom, The stiffness of normal articular cartilage and the predominant acting stress levels: implications for the aetiology of osteoarthrosis, Rheumatology 32 (1) (1993) 16–25, https://doi.org/10.1093/rheumatology/32. 1.16.

[33] T. Lyyra, I. Kiviranta, U. Väätäinen, H.J. Helminen, J.S. Jurvelin, In vivo characterization of indentation stiffness of articular cartilage in the normal human knee, J. Biomed. Mater. Res. A 48 (4) (1999) 482–487, https://doi.org/10.1002/(SICI) 1097-4636(1999)48:4 < 482::AID-JBM13 > 3.0.CO;2-M.

[34] J. Yao, B. Seedhom, Mechanical conditioning of articular cartilage to prevalent stresses, Rheumatology 32 (11) (1993) 956–965, https://doi.org/10.1093/ rheumatology/32.11.956.

[35] L. Burgin, L. Edelsten, R. Aspden, The mechanical and material properties of elderly human articular cartilage subject to impact and slow loading, Med. Eng. Phys. 36 (2) (2014) 226–232, https://doi.org/10.1016/j.medengphy.2013.11.002.

[36] D.L. Robinson, M.E. Kersh, N.C. Walsh, D.C. Ackland, R.N. de Steiger, M.G. Pandy, Mechanical properties of normal and osteoarthritic human articular cartilage, J. Mech. Behav. Biomed. Mater. 61 (2016) 96–109, https://doi.org/10.1016/j.jmbbm. 2016.01.015.

[37] M. Laasanen, J. Töyräs, R. Korhonen, J. Rieppo, S. Saarakkala, M. Nieminen, J. Hirvonen, J. Jurvelin, Biomechanical properties of knee articular cartilage, Biorheology 40 (1, 2, 3) (2003) 133–140.

[38] A. Gannon, T. Nagel, A. Bell, N. Avery, D. Kelly, Postnatal changes to the mechanical properties of articular cartilage are driven by the evolution of its collagen network, Eur. Cell. Mater. 29 (105) (2015) e23.

[39] A.K. Williamson, A.C. Chen, R.L. Sah, Compressive properties and function–composition relationships of developing bovine articular cartilage, J. Orthop. Res. 19 (6) (2001) 1113–1121, https://doi.org/10.1016/S0736-0266(01)00052-3.

[40] K. Hu, L. Xu, L. Cao, C.M. Flahiff, J. Brussiau, K. Ho, L.A. Setton, I. Youn, F. Guilak, B.R. Olsen, Y. Li, Pathogenesis of osteoarthritis-like changes in the joints of mice deficient in type IX collagen, Arthritis Rheum. 54 (9) (2006) 2891–2900, https:// doi.org/10.1002/art.22040.

[41] M.L. Roemhildt, K.M. Coughlin, G.D. Peura, B.C. Fleming, B.D. Beynnon, Material properties of articular cartilage in the rabbit tibial plateau, J. Biomech. 39 (12)

(2006) 2331–2337, https://doi.org/10.1016/j.jbiomech.2005.07.017.

[42] P. Julkunen, T. Harjula, J. Iivarinen, J. Marjanen, K. Seppänen, T. Närhi, J. Arokoski, M.J. Lammi, P.A. Brama, J.S. Jurvelin, H.J. Helminen, Biomechanical, biochemical and structural correlations in immature and mature rabbit articular cartilage, Osteoarthr. Cartil. 17 (12) (2009) 1628–1638, https://doi.org/10.1016/j.joca.2009.07.002.

[43] J.-P. Berteau, M. Oyen, S. Shefelbine, Permeability and shear modulus of articular cartilage in growing mice, Biomech. Model. Mechanobiol. 15. https://doi.org/10.1007/s10237-015-0671-3.

[44] F. Barry, R.E. Boynton, B. Liu, J.M. Murphy, Chondrogenic differentiation of mesenchymal stem cells from bone marrow: differentiation-dependent gene expression of matrix components, Exp. Cell Res. 268 (2) (2001) 189–200, https://doi.org/10.1006/excr.2001.5278.

[45] A.D. Murdoch, L.M. Grady, M.P. Ablett, T. Katopodi, R.S. Meadows, T.E. Hardingham, Chondrogenic differentiation of human bone marrow stem cells in transwell cultures: generation of scaffold-free cartilage, Stem Cells 25 (11) (2007) 2786–2796, https://doi.org/10.1634/stemcells.2007-0374.

[46] K. Pelttari, A. Winter, E. Steck, K. Goetzke, T. Hennig, B.G. Ochs, T. Aigner, W. Richter, Premature induction of hypertrophy during in vitro chondrogenesis of human mesenchymal stem cells correlates with calcification and vascular invasion after ectopic transplantation in SCID mice, Arthritis Rheum. 54 (10) (2006) 3254–3266, https://doi.org/10.1002/art.22136.

[47] A.M. Mackay, S.C. Beck, J.M. Murphy, F.P. Barry, C.O. Chichester, M.F. Pittenger, Chondrogenic differentiation of cultured human mesenchymal stem cells from marrow, Tissue Eng. 4 (4) (1998) 415–428, https://doi.org/10.1089/ten.1998.4.415.

[48] A.J. Engler, S. Sen, H.L. Sweeney, D.E. Discher, Matrix elasticity directs stem cell lineage specification, Cell 126 (4) (2006) 677–689, https://doi.org/10.1016/j.cell.2006.06.044.

[49] J.L. Allen, M.E. Cooke, T. Alliston, ECM stiffness primes the TGFβ pathway to promote chondrocyte differentiation, Mol. Biol. Cell 23 (18) (2012) 3731–3742.

[50] L.A. Taber, Biomechanics of growth, remodeling, and morphogenesis, Appl. Mech. Rev. 48 (8) (1995) 487–545, https://doi.org/10.1115/1.3005109.

[51] A. Goriely, The Mathematics and Mechanics of Biological Growth, 45 Springer, 2017.